Photomedicine and Laser Surgery
Volume 33, Number 9, 2015

Pp. 452–459
DOI: 10.1089/pho.2015.3893

Analysis of Radiomodulatory Effect of Low-Level Laser Irradiation by Clonogenic Survival Assay

Gholamreza Esmaeeli Djavid, MD,[1] Bahram Goliaie, PhD,[1] and Alireza Nikoofar, MD[2]

Abstract

Objective: The aim of this study was to investigate the radiomoulatory effects of low-level laser irradiation (LLLI) in normal and cancer cells exposed to ionizing X-ray radiation on clonogenic survival assay. ***Background data:*** LLLI does have radioprotective effects on normal tissue. LLLI can reduce the incidence of mucocutaneous complications of ionizing radiation. Few *in vitro* studies reported adaptive responses for LLLI to ionizing radiation in normal and cancer cells, particularly with respect to clonogenic cell survival assay. ***Methods:*** Normal NIH 3T3 cells and cancer HeLa cells were irradiated with 685 and 830 nm LLLI at different energy densities prior to ionizing X-ray radiation. The survival fraction was determined after ionizing radiation (0, 2, 4, and 6 Gy). The values of the linear (α) and quadratic (β) parameters were calculated based on the clonogenic survival curves. ***Results:*** Clonogenic radiation survival assay showed that the application of LLLI at 685 nm prior to ionizing radiation could significantly inhibit clonogenic growth of HeLa cells compared with unirradiated HeLa cells. LLLI could also significantly increase the α parameter of the linear quadratic (LQ) model. In contrast, application of LLLI at 830 nm could significantly protect NIH 3T3 cells against radiation and decreased α parameter. ***Conclusions:*** This study suggests that various physical parameters of LLLI can be diverse adaptive responses to ionizing radiation on normal and cancer cells.

Introduction

RADIOTHERAPY PLAYS A CRITICAL ROLE in management of cancer treatment through ionizing radiation. The radiotherapy outcome is often limited by radioresistance in cancer cells and side effects in normal cells and tissues.[1] The cytotoxic effect of ionizing radiation is mainly caused by DNA damages, including single and double strand breaks (SSBs and DSBs), sugar and base modifications, and DNA–protein crosslinks.[2] The DSBs are dominant forms of DNA damage and may lead to cell death following radiation.[3] Loss of reproductive integrity and proliferation inability are the most common features of cell death following ionizing radiation,[4–6] which may refer to reproductive death or clonogenic cell death. Therefore, the clonogenic cell survival assays have been played an essential role in the study of ionizing radiation effects, and is the primary end-point measured in radiobiology.[3]

There have been many attempts to improve the therapeutic effects of radiotherapy by selective protection of normal cells without radioresistance effects in cancer cells, such as dose-fractionation of radiotherapy.[7] Chemical and physical approaches to radioprotection of normal cells have been developed to increase radiation efficiency. Researchers have tried to prevent death in normal cells following ionizing radiation.[8–14] These approaches probably do not enhance radioresistance characteristics in cancer cells and cannot help to develop radiation-induced secondary cancers.[1] Also, the approaches mentioned help to protect normal cells from ionizing radiation or induce radiosensitization of cancer cells. These methods have been reported to be effective based on the presumption of the apoptotic cell loss as the central event in radiotherapy's early outcome.[1,8]

Low-level laser therapy, also known as photobiomodulation, employs visible or near-infrared light (600–1000 nm) to treat various injuries or pathologies in humans or animals.[15–18] There is strong evidence showing that low-level laser irradiation (LLLI) is absorbed in mitochondria of mammalian cells, particularly by cytochrome c oxidase.[19,20] Consequently, a cascade of events occurs in the mitochondria leading to biostimulation of various processes affecting the molecular and cellular levels at different types of cells. LLLI alters the cellular redox state, which induces the activation of numerous intracellular signaling pathways, and alters the affinity of transcription factors involved in cell proliferation, survival, and tissue repair and regeneration.[21–23] It has been

[1]Laboratory of Biophysics and Molecular Biology, Institute of Biochemistry and Biophysics (IBB), University of Tehran, Tehran, Iran.
[2]Radiotherapy Department, Firoozgar Hospital, Iran University of Medical Sciences. Tehran, Iran.

proposed that LLLI could be capable of protecting cells against some cytotoxic agents such as ionizing radiation. In addition, LLLI has a biphasic dose-response pattern.[24] This stimulatory effect of laser irradiation has been reported at low energy densities (fluences), but there has also been an inhibitory effect reported at higher energy densities. The higher energy density of laser irradiation interferes with cell cycling and inhibition of cell proliferation.[25,26] As a result, LLLI could possibly increase cell sensitization to ionizing radiation in a paradoxical manner.

There are many clinical reports that support the radioprotective effects of LLLI in normal tissue,[27–29] which can reduce the incidence of radiotherapy-induced mucocutaneous complications, such as oral mucositis and dermatitis. LLLI can also modulate subcellular signaling pathways, and may lead to increased cell resistance to ionizing radiation. For example, LLLI induces downregulation of p53 activity and increases the activity of nuclear factor kappa-B (NF-kB) protein, both leading to cell survival.[22,30,31] Despite of the mentioned evidence, few *in vitro* studies reported that LLLI causes adaptive responses to ionizing radiation in normal and cancer cells. Clonogenic cell survival assay and its survival curves have wide application in evaluating the reproductive integrity of different cells, and describe a relationship between the ionizing radiation dose and the proportion of surviving cells. As a result, it is crucial to conduct a study to evaluate the modifying effects of LLLI on ionizing radiation survival curves, both in normal and cancer cells that were pre-exposed to LLLI.[32] Our study was conducted to evaluate and compare the adaptive responses of LLLI on ionizing radiation cell survival curves in normal and cancer cells.

Materials and Methods

Cell line and culture conditions

Experiments were conducted with HeLa cells (human cervix carcinoma; ATCC® CCL-2™) and NIH 3T3 cells (NIH Swiss mouse embryonic fibroblasts; ATCC CRL 1658™). Cells were purchased from National Cell Bank of Iran (Pasteur Institute, Iran). The two cell lines were cultured in RPMI-1640 medium (Gibco®, UK), supplemented with 10% fetal bovine serum (Gibco) and 100 U/mL Penicillin (Sigma, USA), and 100 μg/mL Streptomycin (Jaber-ebn-Hayan, Tehran, Iran) at 37°C with 5% CO_2 in humidified air. The cells were passaged using 0.25% trypsin and 0.03% ethylenediaminetetraacetic acid (EDTA) (Sigma) in phosphate buffered saline (PBS) solution.

LLLI

The cells were directly exposed to various wavelengths and energy densities of laser light that were chosen according to commonly applied energy densities for laser therapies. A summary of the laser parameters is shown in Table 1. The BTL-5000 laser series was used for the laser irradiation. This device was specifically designed to provide uniform irradiation to the culture plates on which the cells were seeded, according to the parameters established for the study. The reduction in power density caused by this type of irradiation was calculated using a laser power meter (ThorLab PM100A, USA). HeLa and NIH 3T3 cells were exposed to either 1 or 5 J/cm^2 with 685 or 830 nm laser light 24 h after seeding, whereas control cells received 0 J/cm^2. The area of exposure was held constant, and included the entire area of the colonies on the culture plates.

Plotting of the growth curve and measurement of the doubling time

HeLa and NIH 3T3 were seeded at a density of 2×10^4 cell/cm^2 in 96 well plates in triplicate. The cells were harvested and counted using the trypan blue dye exclusion method. Viable cells in three wells of each group were counted for 7 consecutive days. The culture medium was exchanged every 3 days. The doubling time (Td) of each cell line was calculated according to the Patterson formula as follow:[33]

$$T_d = T \times \log 2 / \log\left(\frac{N_2}{N_1}\right)$$

where N_1 is cell number on the 1st day of the exponential phase, and N_2 is cell number at T h after culture (end of exponential phase); T (h) is the time from N_1 to N_2.

MTT cell viability assay

Cell proliferation was evaluated using the tetrazolium salt (MTT) method. MTT is useful for the quantification of viable cells, because only metabolically active cells cleave it to form a formazan dye. In exponential phase of cell growth, HeLa and NIH 3T3 cells were trypsinized and seeded at an initial density of 1×10^4 cells/cm^2 in 96 well plates. After 24 h, the cells were irradiated with 0, 1, 5, and 10 J/cm^2 at 685 or 830 nm. After 48 h, medium was removed from each well, and 50 mL MTT solution (Sigma, USA) (2 mg/mL PBS) was added to each well. Cells were incubated at 37°C for 3 h to let

Table 1. Summary of Laser and X-Ray Parameters Used in this Study

Low-level laser irradiation parameters		*X-ray ionizing radiation parameters*	
Laser system	*BTL-5000*	*X-ray generator*	*Siemens Primus linear accelerator*
Wavelength (nm)	685, 830	photon energy (MeV)	6
Irradiation mode	Continuous	Dose rate (cGy/min)	200
Power output (mW)	50	Dose (Gy)	2, 4, 6
Power density (mW/cm^2)	16		
Energy density (J/cm^2)	1, 5		
Duration of irradiation (s): 1 J/cm^2	60		
5 J/cm^2	300		

formazan crystals accumulate. The medium was removed, and formazan crystals were solubilized through addition of 100 mL dimethyl sulfoxide (DMSO) to each well. Absorbance at 570 and 630 nm wavelengths was measured with a BioTek plate reader. Difference of absorbance at the two wavelengths represented cell viability.

Plating efficiency assay

Exponential growing cells were trypsinized and plated at 200 cells/well density into 12 well plates, and allowed to adhere overnight. Each well was irradiated with 685 and 830 nm wavelengths at 0, 1, and 5 J/cm^2 energy densities at 24 h after seeding. After 9 days in culture, the cells were fixed in 2% formaldehyde and stained with crystal violet (0.5%). The number of colonies containing at least 50 cells was counted under a light microscope (Leica, DMLS).

Clonogenic survival assays

The clonogenic assay protocol is described in Fig. 1. Cells were trypsinized and counted carefully and diluted such that appropriate cell numbers were seeded into each well of 12 well plates. It is statistically necessary to plate enough cells to obtain a colony count of 20–100. For example, this may require only 100 cells for the control plate (0 Gy ionizing radiation), whereas at 6 Gy, this may require ≥ 800 cells. In this study, the cells were plated in 12 well plates at 200, 400, 600, and 800 cells per well, at 0, 2, 4, and 6 Gy ionizing radiation doses, respectively, and incubated overnight. The cells were pre-exposed to LLLI at 0, 1, and 5 J/cm^2 with 685 and 830 nm wavelengths. After 1 h incubation, the cells were irradiated at room temperature with 6 MeV X-ray photons from a Siemens Primus linear accelerator (Germany) at a dose rate of 200 cGy/min (Table 1). After incubation for 8–9 days, the colonies were fixed and stained as described. The survival fraction was calculated as the ratio between the colonies formed after ionizing irradiation and the number of cell seeded with a correction for the plating efficiency.[34]

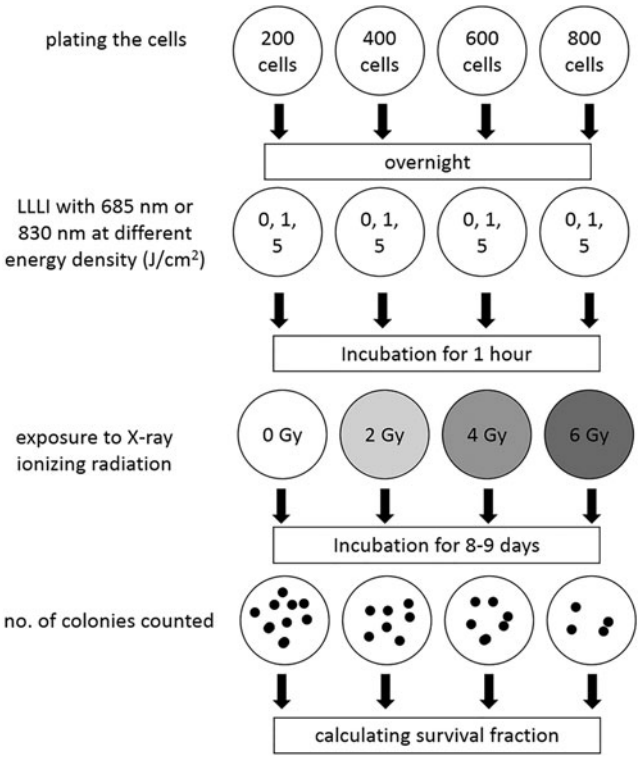

FIG. 1. Schematic representation of the major steps involved in a typical clonogenic cell survival assay.

Analysis of the radiation dose survival curve

In this study, dose-response radiation survival curve was mathematically analyzed based on the linear quadratic (LQ) model of cell reproductive death as a function of ionizing radiation dose.[34] In this model, the surviving fraction (S_D) of cells after a radiation dose (D) was fit by a weighted, stratified, linear regression described by an inverse exponential approximation:

$$S_D/S_0 = e^{-(\alpha D + \beta D^2)}$$

The LQ model contains two parameters, α (Gy^{-1}) and β (Gy^{-2}). Parameter α represents the initial slope of cell dose-survival curves and the effectiveness of radiation at low doses, whereas the quadratic parameter β represents the increasing contribution from cumulative damage, presumably caused by the interaction of two or more lesions induced by

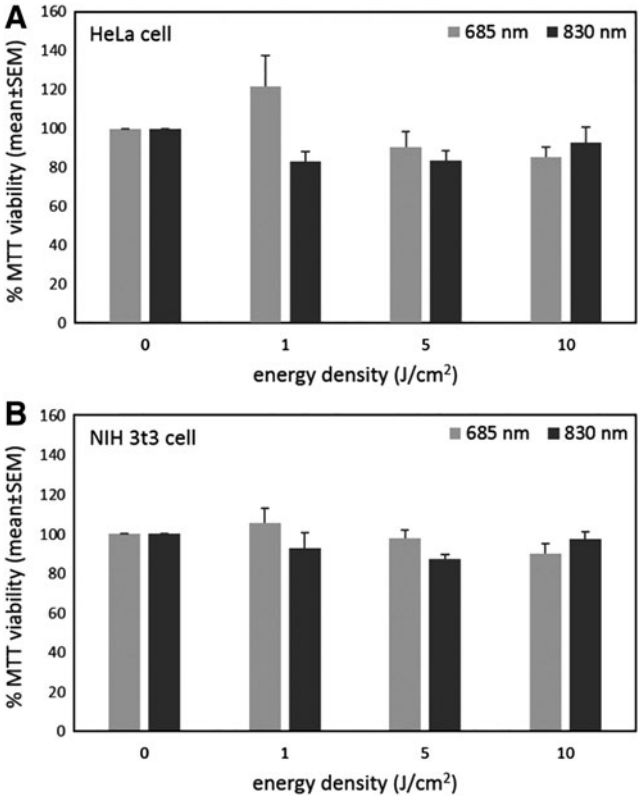

FIG. 2. MTT assay of HeLa **(A)** and NIH 3T3 **(B)** cells in different wavelengths and energy densities of low-level laser irradiation (LLLI). Means with standard errors of at least three independent experiments performed in triplicate are shown.

separate ionizing radiations. The parameters α and β were determined from survival curves using SPSS 17 (Chicago, IL) statistical software performing a fit to the data according to the LQ formula by multiple regression analysis.

Statistical analysis

Statistical analyses were performed using SPSS 17 software. Data are presented as means ± standard error of mean (SEM). For continuous variables, means were compared by one way analysis of variance (ANOVA) and Tukey's post-hoc testing. The level of statistical significance was set at a two tailed p value of 0.05.

Results

Growth curve and doubling time

Because the doubling time is the time required for each doubling of cell growth/count in the exponential phase, it can be an important parameter in estimating time required for cell proliferation rate and colony formation. In this study, the baseline doubling times in HeLa and NIH 3T3 cells were 28.7 ± 1.7 and 22.2 ± 0.7, respectively. It means that the proliferation rate of NIH 3T3 cell is significantly more than the HeLa cell proliferation rate ($p < 0.001$).

Cell viability assay

The viability of HeLa and NIH 3T3 cells to 685 and 830 nm LLLI is shown in Fig. 2. At 685 nm of LLLI, 1 J/cm^2 energy density increased viability of Hela cells, whereas there was no significant effect of other energy densities (Fig. 2A). LLLI with 685 and 830 nm at different energy densities did not influence the viability of NIH 3T3 cells (Fig. 2B).

Plating efficiency assay

Plating efficiency is typically used to describe growth properties of cells *in vitro*. The plating efficiency of HeLa cell significantly enhanced after exposure to LLLI at energy densities 1 and 5 J/cm^2 with 685 and 830 nm (Fig. 3A). The plating efficiency of NIH 3T3 cell exposed to 1 J/cm^2 LLLI with 685 and 830 nm was increased, whereas LLLI at 5 J/cm^2 energy density did not substantially affect the plating efficiency in NIH 3T3 cells (Fig. 3B).

Clonogenic survival assays

The ionizing radiation was performed *in vitro* 60 min after the cells were pre-exposed to LLLI. The radiation sensitization of HeLa and NIH 3T3 cells with or without being pre-exposed to LLLI was described as changes in linear and

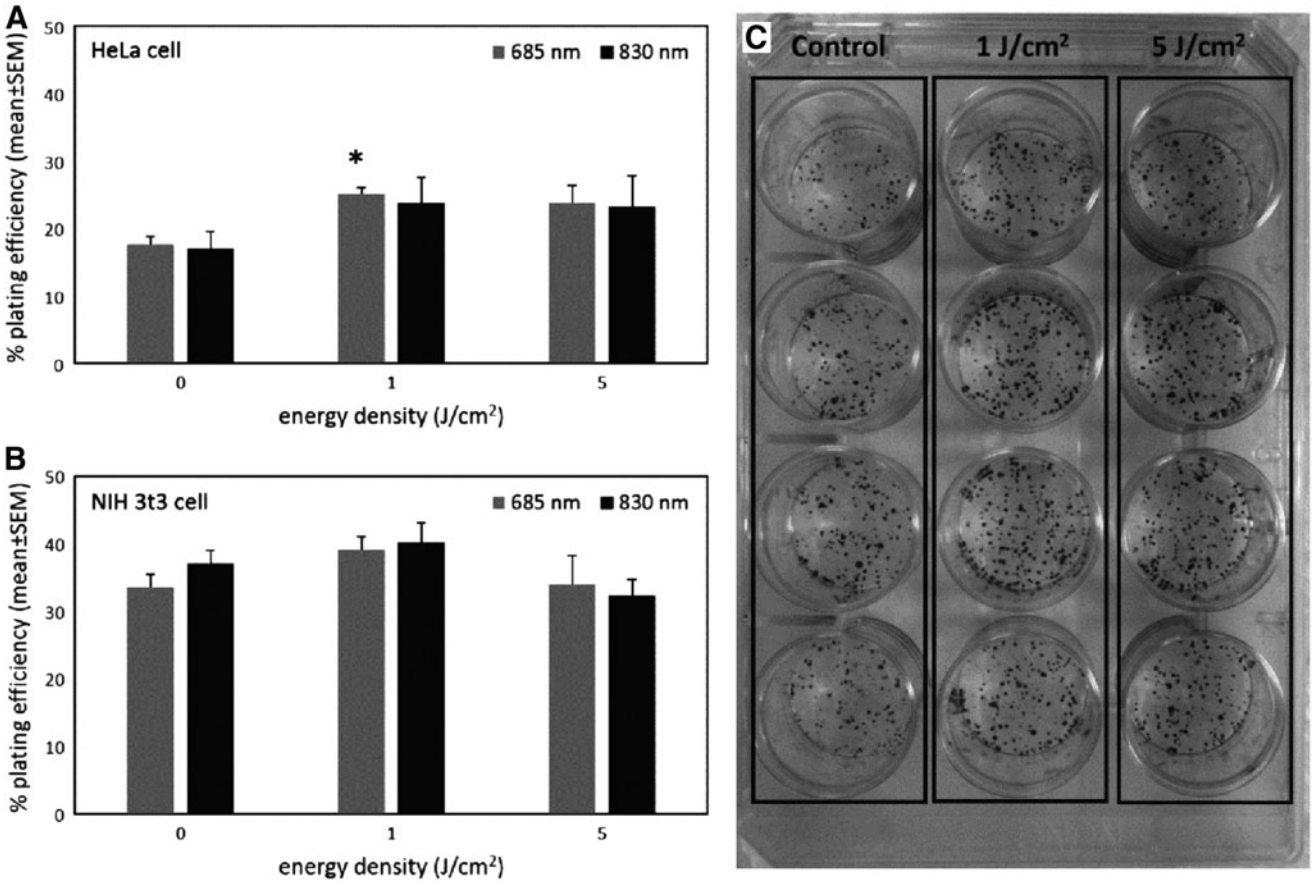

FIG. 3. Plating efficiency of HeLa **(A)** and NIH 3T3 **(B)** cells after exposure to low-level laser irradiation (LLLI) in different wavelengths and power densities. LLLI at 1 J/cm^2 with 685 nm had a significant stimulatory effect on plating efficiency in HeLa cells **(A)**. Means with standard errors of at least three independent experiments performed in triplicate are shown. *$p < 0.05$ compared with the corresponding control. Representative colonies of HeLa cells are shown **(C)**.

quadratic parameters of radiation dose-survival curves. In Fig. 4A and B, the ionizing radiation survival curves are shown for HeLa cells pre-exposed to LLLI at 685 and 830 nm wavelengths, respectively. In Fig. 4A, a statistically significant increase in the radiosensitivity was observed in HeLa cells that were pre-exposed to 685 nm LLLI at 5 J/cm^2 energy density ($p < 0.01$). Pre-exposure to LLLI at both energy densities with 830 nm did not significantly effect the ionizing radiation survival curves of HeLa cells (Fig. 4B).

In Fig. 5A and B, the ionizing radiation survival curves are shown for NIH 3T3 cells pre-exposured to LLLI with 685 and 830 nm wavelengths, respectively. In Fig. 5A, the survival curves of NIH 3T3 cells pre-exposed to LLLI at both energy densities with 685 nm were the same as those for control NIH 3T3 cells. On the other hand, LLLI at 1 J/cm^2 with 830 nm led to a significantly higher cell survival

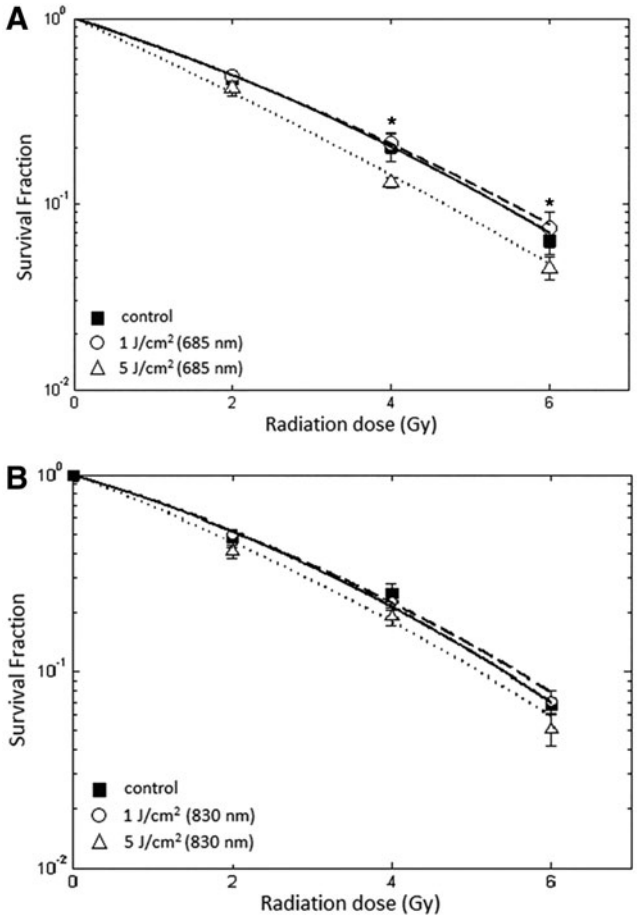

FIG. 4. Radiation survival curves of HeLa cells after being pre-exposed to low-level laser irradiation (LLLI). The cells were illuminated by LLLI at 1 and 5 J/cm^2 with 685 and 830 nm wavelengths. One hour later, cells were radiated with different doses of ionizing radiation. LLLI at 5 J/cm^2 with 685 nm significantly sensitized HeLa cell to ionizing radiation **(A)**. The radiation survival curve of HeLa cells after being pre-exposed to 830 nm LLLI was not significantly different **(B)**. Survival data were fitted to the linear quadratic model. Error bar indicates standard error of the mean of at least three independent experiments in triplicate. *$p < 0.05$ compared with the corresponding control.

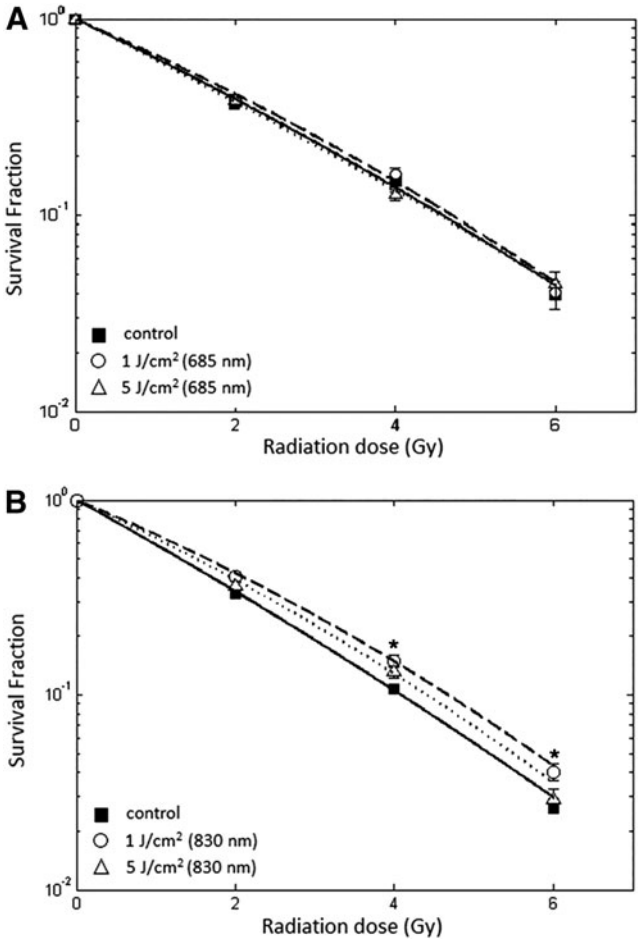

FIG. 5. Radiation survival curves of NIH 3T3 cells after being pre-exposed to low-level laser irradiation (LLLI). The cells were illuminated by LLLI at 1 and 5 J/cm^2 with 685 and 830 nm wavelengths. One hour later, cells were exposed to different doses of ionizing radiation. The radiation survival curves of NIH 3T3 cells after being pre-exposed to 685 nm LLLI were not significantly different **(A)**. LLLI at 1 J/cm^2 with 850 nm significantly increased the survival fraction of NIH 3T3 to ionizing radiation **(B)**. Survival data were fitted to the linear quadratic model. Error bar indicates standard error of mean of at least three independent experiments in triplicate. *$p < 0.05$ compared with the corresponding control.

in NIH 3T3 cells, whereas LLLI at 5 J/cm^2 could not statistically alter NIH 3T3 cell survival curve in comparison with control NIH 3T3 cells (Fig. 5B).

The effects of LLLI on the LQ parameters are summarized in Table 2. There was a significant increase in parameter α value in HeLa cells pre-exposed to LLLI at 5 J/cm^2 energy density with 685 nm. In contrast, there was a significant reduction in parameter α value in NIH 3T3 cells exposed to LLLI at 1 J/cm^2 energy density with 830 nm (Table 2). For both energy densities and wavelengths of LLLI, there were no statistically significant differences between β values and control HeLa and NIH 3T3 cells ($p > 0.05$).

Discussion

The common therapeutic doses of ionizing radiation therapy are in range of 1.5–2.5 Gy.[35] Parameter α, the initial

Table 2. Values of the Linear Quadratic Parameters α and β from HeLa and NIH 3T3 Cells Treated with Ionizing Radiation After Pre-Exposure to LLLI

		685 nm		830 nm	
Cells	*Treatment*	α (Gy^{-1})	β (Gy^{-2})	α (Gy^{-1})	β (Gy^{-2})
HeLa	Control	0.31 ± 0.04	0.02 ± 0.01	0.27 ± 0.06	0.03 ± 0.06
	1 J/cm^2	0.32 ± 0.04	0.02 ± 0.01	0.28 ± 0.05	0.02 ± 0.01
	5 J/cm^2	0.45 ± 0.05[a]	0.01 ± 0.01	0.35 ± 0.06	0.02 ± 0.01
NIH 3T3	Control	0.45 ± 0.05	0.012 ± 0.01	0.52 ± 0.02	0.01 ± 0.006
	1 J/cm^2	0.41 ± 0.04	0.01 ± 0.009	0.38 ± 0.03[a]	0.02 ± 0.007
	5 J/cm^2	0.49 ± 0.05	0.007 ± 0.009	0.43 ± 0.04	0.02 ± 0.01

Error bar indicates standard error of mean of three independent experiments.
LLLI, low-level laser irradiation.
[a]$p < 0.01$ compared with the corresponding control.

slope of radiation dose-survival curves, is mainly related to clinical efficacy of radiation therapy. In our study, α value was increased while HeLa cancer cells were pre-exposed to LLLI at a higher energy density (5 J/cm^2) with a 685 nm wavelength. We assumed that LLLI could enhance direct potentially lethal damage (PDL) at low ionizing radiation doses, and lead to hypersensitizing HeLa cells to ionizing radiation. The level of survival fraction might decrease in HeLa cells pre-exposed to 5 J/cm^2 LLLI with 685 nm. The mentioned phenomena provide another example of radiosensitization effects in HeLa cells. In contrast, the α value in a NIH 3T3 normal cell survival curve decreased when these cells were pre-exposed to the lower energy density (1 J/cm^2) of LLLI with 830 nm wavelength. This means that the 830 nm LLLI had a radioprotective effect on NIH 3T3 cells. The significant increase in the levels of SF2, SF4, and SF6 in NIH 3T3 cells that were exposed to 830 nm LLLI at 1 J/cm^2 validates this radioprotection. The changes of the β component presumably depend on the interaction of reparable sublethal damage. These changes were not significantly different between both cell types and laser parameters.

The critical question is explaining the various effects of the LLLI. Dose-response of LLLI depends on cell types and illumination parameters such as wavelength, power density, energy density, pulse structure, and treatment timing.[36–38] The dose-response effect of the LLLI is biphasic.[24] Lower energy densities of LLLI have a beneficial effect on stimulating and repairing cells and tissues, but higher energy densities have inhibitory effects, such as induction of apoptosis. The mechanism of the biphasic dose-response effect can be explained through production of reactive oxygen species (ROS) by mitochondria following LLLI.[15,26] LLLI provides an oxidative stress and generates ROS in biological systems, which are quenched by cellular antioxidant systems.[22] ROS homeostasis and signaling have an important role in cell signaling following adaptive response, particularly to ionizing radiation.[39] The ROS generated by LLLI may escape from antioxidant systems, cause redox imbalance, and activate redox-sensitive signaling factors such as nuclear factor κB (NF-κB).[40,41] LLLI at lower stimulatory energy densities inhibits apoptosis through Akt/GSK3beta signaling pathways.[42] All these mechanisms can finally lead cellular response to induce radioprotection effects. It has been shown that 685 nm of LLLI at very low energy densities (0.01 J/cm^2) enhances cell survival to γ-ionizing radiation.[43] Increasing energy densities of LLLI causes a large amount of oxidative stress and ROS formation in relative cytotoxic levels. Cytotoxic levels of ROS raise various types of cellular damage and induce apoptosis via generation of high levels of ROS and via Akt/GSK3beta signaling pathways.[25,26,44] The apoptosis induced by high energy densities of LLLI was directly initiated from mitochondrial ROS generation, decrease in mitochondrial membrane potential, and other ROS-dependent pathways.[24,44,45] LLLI at higher energy densities can also enhance cell death caused by ionizing radiation and radiosensitizing HeLa cells. The radiomodulatory effect of LLLI with a higher energy density may be also explained by the ROS homeostasis. The boundaries between lower stimulatory and higher inhibitory energy densities of LLLI are still controversial.

The radiomodulatory effects of LLLI were obtained on exponentially growing HeLa and NIH 3T3 cells. The increased DNA damage is the major component of radiosensitisation in exponentially growing cells. Meanwhile, in plateau phase cells, radiosensitisation occurs through inhibited repair and/or enhanced fixation of potentially lethal damage.[35] The DNA damage, particularly the DSBs, can lead to cell death following radiation.[3] The α value increase for exponentially growing HeLa cells pre-exposed to LLLI at 5 J/cm^2 energy densities with 685 nm leads to an increase in the number of directly lethal events caused by the LLLI. Former research has shown that LLLI at higher energy densities enhanced DNA damage compared with unirradiated cells.[46,47] Based on the ''law of Bergonié and Tribondeau'' in radiobiology, radiosensitivity of cells helps to increase the level of metabolic activity and the proliferation rate. A significant increase of plating efficiency in HeLa cells represents cell proliferation caused by LLLI. This process shows that more time is necessary to determine the proliferative effect of LLLI. Obviously, a period of 8–9 days for colony formation provides enough time to show the stimulatory effect of the LLLI.

Conclusions

There is growing interest in using LLLI as a safe approach to prevent ionizing radiation induced side effects, such as oral mucositis and dermatitis. However, there is still a need for a safe treatment approach without the disadvantages of radioresistance to remaining cancer cells.[48] The aim of this study was focused on analysis of the ionizing

radiation survival curve in cells pre-exposed to different parameters of LLLI. In conclusion, the results of this study demonstrate a possible radiosensitizing effect for 685 nm LLLI in HeLa cancer cells, evidenced by decreased survival fraction and increased α value according to the LQ model at 5 J/cm^2 energy density. However, the radioprotection effect of 830 nm LLLI at lower energy densities (1 J/cm^2) was observed in NIH 3T3 normal cells. Based on our finding, it is necessary to provide more research on relevant *in vitro* studies and clinical trials to identify radiomodulatory effects and the mechanism of LLLI inside human bodies.

Author Disclosure Statement

No competing financial interests exist.

References

1. Gudkov AV, Komarova EA. Radioprotection: smart games with death. J Clin Invest 2010;120:2270–2273.
2. Roots R, Kraft G, Gosschalk E. The formation of radiation-induced DNA breaks: the ratio of double-strand breaks to single-strand breaks. Int J Radiat Oncol Biol Phys 1985; 11:259–265.
3. Denekamp J. Cell kinetics and radiation biology. Int J Radiat Biol Relat Stud Phys Chem Med 1986;49:357–380.
4. Karin M. Nuclear factor-kappaB in cancer development and progression. Nature 2006;441:431–436.
5. Paris F, Fuks Z, Kang A, et al. Endothelial apoptosis as the primary lesion initiating intestinal radiation damage in mice. Science 2001;293:293–297.
6. Vousden KH, Prives C. Blinded by the light: the growing complexity of p53. Cell 2009;137:413–431.
7. Bhide SA, Nutting CM. Recent advances in radiotherapy. BMC Med 2010;8:25.
8. Jorgensen TJ. Enhancing radiosensitivity: targeting the DNA repair pathways. Cancer Biol Ther 2009;8,:665–670.
9. Rosenberg A, Knox S. Radiation sensitization with redox modulators: a promising approach. Int J Radiat Oncol Biol Phys 2006;64:343–354.
10. Wardman P. Chemical radiosensitizers for use in radiotherapy. Clin Oncol 2007;19:397–417.
11. Goliaei B, Rajabi H, Rabbani A. Effects of hyperthermia on the colony-stimulating factor production by the lung. Int J Radiat Oncol Biol Phys 1992;22:1029–1033.
12. Keshmiri–Neghab H, Goliaei B, Nikoofar A. Gossypol enhances radiation induced autophagy in glioblastoma multiforme. Gen Physiol Biophys 2014;33:433–442.
13. Rouhani M, Goliaei B, Khodagholi F, Nikoofar A. Lithium increases radiosensitivity by abrogating DNA repair in breast cancer spheroid culture. Arch Iran Med 2014;17: 352–360.
14. Maier P, Wenz F, Herskind C. Radioprotection of normal tissue cells. Strahlenther Onkol 2014;190:745–752.
15. Chung H, Dai T, Sharma SK, Huang YY, Carroll JD, Hamblin MR. The nuts and bolts of low-level laser (light) therapy. Ann Biomed Eng 2012;40:516–533.
16. Bensadoun RJ, Nair RG. Low-level laser therapy in the prevention and treatment of cancer therapy-induced mucositis: 2012 state of the art based on literature review and meta-analysis. Curr Opin Oncol 2012;24:363–370.
17. Djavid GE, Mehrdad R, Ghasemi M, Hasan–Zadeh H, Sotoodeh–Manesh A, Pouryaghoub G. In chronic low back pain, low level laser therapy combined with exercise is more beneficial than exercise alone in the long term: a randomised trial. Aust J Physiother 2007;53:155–160.
18. Kaviani A, Djavid GE, Ataie–Fashtami L, et al. A randomized clinical trial on the effect of low-level laser therapy on chronic diabetic foot wound healing: a preliminary report. Photomed Laser Surg 2011;29:109–114.
19. Karu TI. Mitochondrial signaling in mammalian cells activated by red and near-IR radiation. Photochem Photobiol 2008;84:1091–1099.
20. Tafur J, Mills PJ. Low-intensity light therapy: exploring the role of redox mechanisms. Photomed Laser Surg 2008;26: 323–328.
21. Avci P, Gupta A, Sadasivam M, et al. Low-level laser (light) therapy (LLLT) in skin: stimulating, healing, restoring. Semin Cutan Med Surg 2013;32:41–52.
22. Chen AC, Arany PR, Huang YY, et al. Low-level laser therapy activates NF-kB via generation of reactive oxygen species in mouse embryonic fibroblasts. PLoS One 2011;6: e22453.
23. Schroeder P, Pohl C, Calles C, Marks C, Wild S, Krutmann J. Cellular response to infrared radiation involves retrograde mitochondrial signaling. Free Radic Biol Med 2007; 43:128–135.
24. Huang YY, Sharma SK, Carroll J, Hamblin MR. Biphasic dose response in low level light therapy–an update. Dose Response 2011;9:602–618.
25. Huang L, Wu S, Xing D. High fluence low-power laser irradiation induces apoptosis via inactivation of Akt/GSK3beta signaling pathway. J Cell Physiol 2011;226: 588–601.
26. Sun X, Wu S, Xing D. The reactive oxygen species-Src-Stat3 pathway provokes negative feedback inhibition of apoptosis induced by high-fluence low-power laser irradiation. FEBS J 2010;277:4789–4802.
27. Bensadoun RJ, Nair RG. Efficacy of low-level laser therapy (LLLT) in oral mucositis: what have we learned from randomized studies and meta-analyses? Photomed Laser Surg 2012;30:191–192.
28. Fife D, Rayhan DJ, Behnam S, et al. A randomized, controlled, double-blind study of light emitting diode photomodulation for the prevention of radiation dermatitis in patients with breast cancer. Dermatol Surg 2010;36:1921–1927.
29. Oberoi S, Zamperlini-Netto G, Beyene J, et al. Effect of prophylactic low level laser therapy on oral mucositis: a systematic review and meta-analysis. PLoS One 2014;9: e107418.
30. Gao X, Xing D. Molecular mechanisms of cell proliferation induced by low power laser irradiation. J Biomed Sci 2009; 16:4.
31. Shefer G, Partridge TA, Heslop L, Gross JG, Oron U, Halevy O. Low-energy laser irradiation promotes the survival and cell cycle entry of skeletal muscle satellite cells. J. Cell Sci 2002;115:1461–1469.
32. Barendsen GW. Parameters of linear-quadratic radiation dose-effect relationships: dependence on LET and mechanisms of reproductive cell death. Int J Radiat Biol 1997; 71:649–655.
33. Zhong X, Xiong M, Meng X, Gong R. Comparison of the multi-drug resistant human hepatocellular carcinoma cell line Bel-7402/ADM model established by three methods. J Exp Clin Cancer Res 2010;29:115.
34. Franken NA, Rodermond HM, Stap J, Haveman J, van Bree C. Clonogenic assay of cells in vitro. Nat Protoc 2006;1: 2315–2319.

35. Franken NA, Oei AL, Kok HP, et al. Cell survival and radiosensitisation: modulation of the linear and quadratic parameters of the LQ model (Review). Int J Oncol 2013; 42:1501–1515.
36. Albuquerque–Pontes GM, Vieira RD, Tomazoni SS, et al. Effect of pre-irradiation with different doses, wavelengths, and application intervals of low-level laser therapy on cytochrome c oxidase activity in intact skeletal muscle of rats. Lasers Med Sci 2015;30:59–66.
37. Djavid GE, Erfani R, Amoohashemi N, Pazouki M, Aghaee S, Pazokitroudi H. Effect of low level He-Ne laser on acute mucosal ulceration induced by indomethacine in rat. Proc SPIE 2002;4903:189–192.
38. Schwartz-Filho HO, Reimer AC, Marcantonio C, Marcantonio E Jr, Marcantonio RA. Effects of low-level laser therapy (685 nm) at different doses in osteogenic cell cultures. Lasers Med Sci 2011;26:539–543.
39. Miura Y. Oxidative stress, radiation-adaptive responses, and aging. J Radiat Res 2004;45:357–372.
40. Droge W. Free radicals in the physiological control of cell function. Physiol Rev 2002;82:47–95.
41. Guo G, Yan–Sanders Y, Lyn-Cook BD, et al. Manganese superoxide dismutase-mediated gene expression in radiation-induced adaptive responses. Mol Cell Biol 2003;23: 2362–2378.
42. Zhang L, Zhang Y, Xing D. LPLI inhibits apoptosis upstream of Bax translocation via a GSK-3beta-inactivation mechanism. J Cell Physiol 2010;224:218–228.
43. Karu T, Pyatibrat L, Kalendo G. Irradiation with He–Ne laser can influence the cytotoxic response of HeLa cells to ionizing radiation. Int J Radiat Biol 1994;65:691–697.
44. Wu S, Xing D, Gao X, Chen WR. High fluence low-power laser irradiation induces mitochondrial permeability transition mediated by reactive oxygen species. J Cell Physiol 2009;218:603–611.
45. Wu S, Xing D, Wang F, Chen T, Chen WR. Mechanistic study of apoptosis induced by high-fluence low-power laser irradiation using fluorescence imaging techniques. J Biomed Opt 2007;12:064015.
46. Biasibetti M, Rojas DB, Hentschke VS, et al. The influence of low-level laser therapy on parameters of oxidative stress and DNA damage on muscle and plasma in rats with heart failure. Lasers Med Sci 2014;29, 1895–1906.
47. Mbene AB, Houreld NN, Abrahamse H. DNA damage after phototherapy in wounded fibroblast cells irradiated with 16 J/cm(2). J Photochem Photobiol B 2009;94:131–137.
48. Sperandio FF, Giudice FS, Correa L, Pinto DS, Jr, Hamblin MR, de Sousa SC. Low-level laser therapy can produce increased aggressiveness of dysplastic and oral cancer cell lines by modulation of Akt/mTOR signaling pathway. J Biophotonics 2013;6:839–847.

Address correspondence to:
Bahram Goliaie
Laboratory of Biophysics and Molecular Biology
Institute of Biochemistry and Biophysics (IBB)
University of Tehran
P.O. Box: 13145-1384
Tehran, Iran

E-mail: goliaei@ibb.ut.ac.ir